

Electrochemical investigation of the substitution reactions of the solvent-coordinated acyl complexes $\eta_5\text{-Cp}(\text{acetone})(\text{CO})\text{FeCOMe}_0^+$ involving thio ethers. Applications of the quantitative analysis of ligand effects

Audrey A. Tracey, Klaas Eriks, Alfred Prock, and Warren P. Giering

Organometallics, **1990**, 9 (5), 1399-1405 • DOI: 10.1021/om00119a008 • Publication Date (Web): 01 May 2002

Downloaded from <http://pubs.acs.org> on March 8, 2009

More About This Article

The permalink <http://dx.doi.org/10.1021/om00119a008> provides access to:

- Links to articles and content related to this article
- Copyright permission to reproduce figures and/or text from this article



ACS Publications
High quality. High impact.

Organometallics is published by the American Chemical Society. 1155 Sixteenth Street N.W., Washington, DC 20036

contributions from π -overlap.

Acknowledgment. We thank the Deutsche Forschungsgemeinschaft and the Fonds der Chemischen Industrie for financial support and Professor H. Schumann and M. Dettlaff, Technical University Berlin, for recording ^{77}Se NMR spectra.

Registry No. 1, 126083-46-3; 3, 20875-32-5; 4, 126109-80-6; 5, 126083-45-2; GeCl_2 -dioxane, 28595-67-7; $\text{W}(\text{CO})_5\text{THF}$, 36477-75-5.

Supplementary Material Available: Tables of U_{ij} values and bond lengths and angles (14 pages); a listing of F_o/F_c values (31 pages). Ordering information is given on any current masthead page.

Electrochemical Investigation of the Substitution Reactions of the Solvent-Coordinated Acyl Complexes $\eta\text{-Cp}(\text{AC})(\text{CO})\text{FeCOMe}^{0,+}$ Involving Thioethers. Applications of the Quantitative Analysis of Ligand Effects

Audrey A. Tracey, Klaas Eriks,* Alfred Prock,* and Warren P. Giering*

Department of Chemistry, Metcalf Center for Science and Engineering, Boston University, Boston, Massachusetts 02215

Received August 1, 1989

The displacement of acetone from $\eta\text{-Cp}(\text{AC})(\text{CO})\text{FeCOMe}^{0,+}$ by thioethers (SMe_2 , SEt_2 , $\text{S}(\text{Ph})\text{Me}$, $\text{S}(\text{Ph})\text{Et}$, SBu_2 , SPh_2 , $\text{S}(\text{i-Pr})_2$, $\text{S}(\text{t-Bu})_2$) at -41°C has been studied by square-wave voltammetry (SWV) coupled with computer simulation. The kinetic data were analyzed and interpreted via the quantitative analysis of ligand effects (QALE). A set of stereoelectronic parameters (χ^s and θ^s) for the thioethers was constructed by transference of the appropriate properties of the phosphorus(III) compounds to the sulfur compounds. It appears that substitution in the iron(III) state occurs via an associative ligand-dependent reaction whose rate depends on both electronic and steric factors. In the iron(II) state the substitution reaction occurs via a preequilibrium dissociative process. The iron(II) reaction is insensitive to the electronic properties of the thioethers but is sensitive to their steric bulk. These results are interpreted in terms of addition of the thioether to the coordinatively unsaturated complex $\eta\text{-Cp}(\text{CO})\text{FeCOMe}$. On the basis of ligand effect data and analysis of the E° values of the $\eta\text{-Cp}(\text{SR}_2)(\text{CO})\text{FeCOMe}^{0,+}$ it is shown that the thioether complexes exhibit steric effects, in contrast to the analogous phosphorus(III) complexes, which show no steric effects.

Introduction

A growing body of evidence indicates that the stoichiometric rearrangement of alkyl metal carbonyls to acyl complexes is assisted by nucleophilic solvents or solutes.¹ The subsequent displacement of the solvent from the resulting weakly solvent-coordinated acyl complex by other potential ligands (metal hydrides, alkenes, alkynes) leads to the downstream chemistry that eventually affords organic products. The solvent-coordinated acyl complexes are clearly key players in this flow of chemistry; however, they are rarely observed and hence difficult to study.

Recently, we demonstrated that the solvent-coordinated complexes $\eta\text{-Cp}(\text{L})(\text{solv})\text{FeCOR}^{0,+}$ are formed *in situ* by low-temperature oxidation of $\eta\text{-Cp}(\text{L})(\text{CO})\text{FeR}$ in coordinating solvents such as acetone (AC),² acetonitrile (AN),³ and methanol.³ These acyl complexes are generally short lived but are amenable to study by electrochemical methods. In electrochemical experiments we have even

seen what appears to be the perchlorate complex, $\eta\text{-Cp}(\text{ClO}_4)(\text{CO})\text{FeCOMe}$, formed from the supporting electrolyte LiClO_4 at -89°C .² In either oxidation state, the complexes are labile although the iron(III) complexes are longer lived than their iron(II) counterparts. This is particularly obvious when $\text{X} = \text{ClO}_4^-$, where the iron(II) complex cannot be observed electrochemically even at -89°C . The greater stability of the iron(III) complexes is probably associated with the hard acid iron(III) complex exhibiting a greater affinity for the hard base solvent.

Through studies with iron(III) acyl complexes (solv = MeOH and AN) we showed that these complexes undergo second-order ligand-dependent substitution reactions of the coordinated solvent.² The MeOH and AN complexes showed less reactivity toward substitution in the iron(II) state at -41°C . When the solvent ligand is acetone, the complexes are more labile, offering the opportunity to study the chemistry of both oxidation states.³ Our initial studies with the acetone complex demonstrated that the solvent ligand was readily displaced by thioanisole at -75°C through a second-order reaction in the iron(III) state. This is probably an entering ligand-dependent reaction, although a preequilibrium dissociative reaction could not be excluded. In the iron(II) state, the substitution clearly follows a two-step rate law indicative of a classical dissociative process. This reactivity toward thioethers offers the opportunity to use ligand effects to gain insight into the stereoelectronic factors that influence the reactivity

(1) (a) Therien, M. J.; Trogler, W. C. *J. Am. Chem. Soc.* 1987, 109, 5127. (b) Webb, S. L.; Giandomenico, C. M.; Halpern, J. *J. Am. Chem. Soc.* 1986, 108, 345. (c) Wax, M. J.; Bergman, R. G. *J. Am. Chem. Soc.* 1981, 103, 7028. (d) Cotton, J. D.; Markwell, R. D. *Organometallics* 1985, 4, 937. (e) Martin, B. D.; Warner, K. E.; Norton, J. R. *J. Am. Chem. Soc.* 1986, 108, 33.

(2) Liu, H.-Y.; Golovin, M. N.; Fertal, D. A.; Tracey, A. A.; Eriks, K.; Giering, W. P.; Prock, A. *Organometallics* 1989, 8, 1454.

(3) Golovin, M. N.; Meiowitz, R. E.; Rahman, Md. M.; Prock, A.; Giering, W. P. *Organometallics* 1987, 6, 2285.

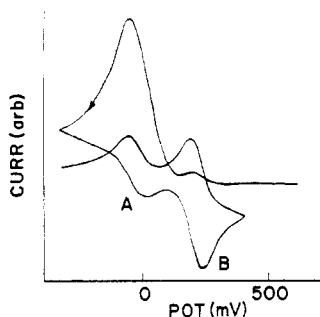


Figure 1. Multiple-sweep cyclic voltammogram of the products resulting from the in situ oxidation of $\eta\text{-Cp}(\text{CO})_2\text{FeMe}$ in acetone containing 0.1 M LiClO_4 and 0.043 M thioanisole at $-41\text{ }^\circ\text{C}$. Initial oxidation was performed at 0.92 V (relative to SCE at $22\text{ }^\circ\text{C}$). Sweep rate was 100 mV s^{-1} . Peaks labeled A and B refer to the anodic waves for the oxidation of $\eta\text{-Cp}(\text{CO})(\text{AC})\text{FeCOMe}$ and $\eta\text{-Cp}(\text{CO})(\text{SPhMe})\text{FeCOMe}$, respectively.

of the solvent-coordinated acyl complexes and to systematically compare the reactivity of isostructural complexes in two oxidation states.

Results

In our previous² paper describing the electrochemistry of $\eta\text{-Cp}(\text{CO})_2\text{FeMe}$ at $-75\text{ }^\circ\text{C}$ in acetone containing thioanisole we reported the formation of species that we identified as the acetone and thioanisole complexes, $\eta\text{-Cp}(\text{AC})(\text{CO})\text{FeCOMe}^{0,+}$ and $\eta\text{-Cp}(\text{CO})(\text{SR}_2)\text{FeCOMe}^{0,+}$. Rate constants for the reactions of this system were extracted from cyclic voltammetry (CV) data.

We have expanded this study and in this paper describe the use of square-wave voltammetry⁴ (SWV) with computer simulation to study the substitution reactions of $\eta\text{-Cp}(\text{CO})(\text{AC})\text{FeCOMe}^{0,+}$ with a variety of thioethers at $-41\text{ }^\circ\text{C}$. SWV offers advantages, among which are high resolution of current waves and consequent ease of analysis. Because the current decays rapidly as potential is swept past a peak, the base line of an experimental SWV curve can be flat even when the sweep is subsequent to a series of potential steps and holds, which cross E° 's of species in solution. We find that we can select a portion of the multiple scan CV experiment and view it at high resolution on a flat base line. (Capacitive currents also have insignificant effects under our experimental conditions.) Figure 1 shows a multiple scan CV for oxidation of $\eta\text{-Cp}(\text{CO})_2\text{FeMe}$ in acetone in the presence of a small amount of SPhMe. The positive return sweep displays current peaks corresponding to oxidation of the neutral acetone ($\eta\text{-Cp}(\text{CO})(\text{AC})\text{FeCOMe}$) and neutral thioether ($\eta\text{-Cp}(\text{CO})(\text{SR}_2)\text{FeCOMe}$) complexes, respectively. This positive return CV sweep may be compared with Figure 4 (vide infra), the corresponding SW voltammogram for a similar positive sweep for SPh₂. Peak heights and half-widths of the SW voltammogram are readily determined with good accuracy for use in computer simulation.

The analysis of the system is based on Scheme I. Substitution or addition reactions can occur in any of three complexes, $\eta\text{-Cp}(\text{CO})_2\text{FeMe}^+$ (or some other closely related and very reactive species) or $\eta\text{-Cp}(\text{AC})(\text{CO})\text{FeCOMe}^{0,+}$. To distinguish between the chemistry of these complexes, we designed a series of electrochemical experiments using tailored wave forms involving a series of steps, holds, and a staircase (with a superimposed square wave). These four wave forms are shown in Figure 2. The square-wave

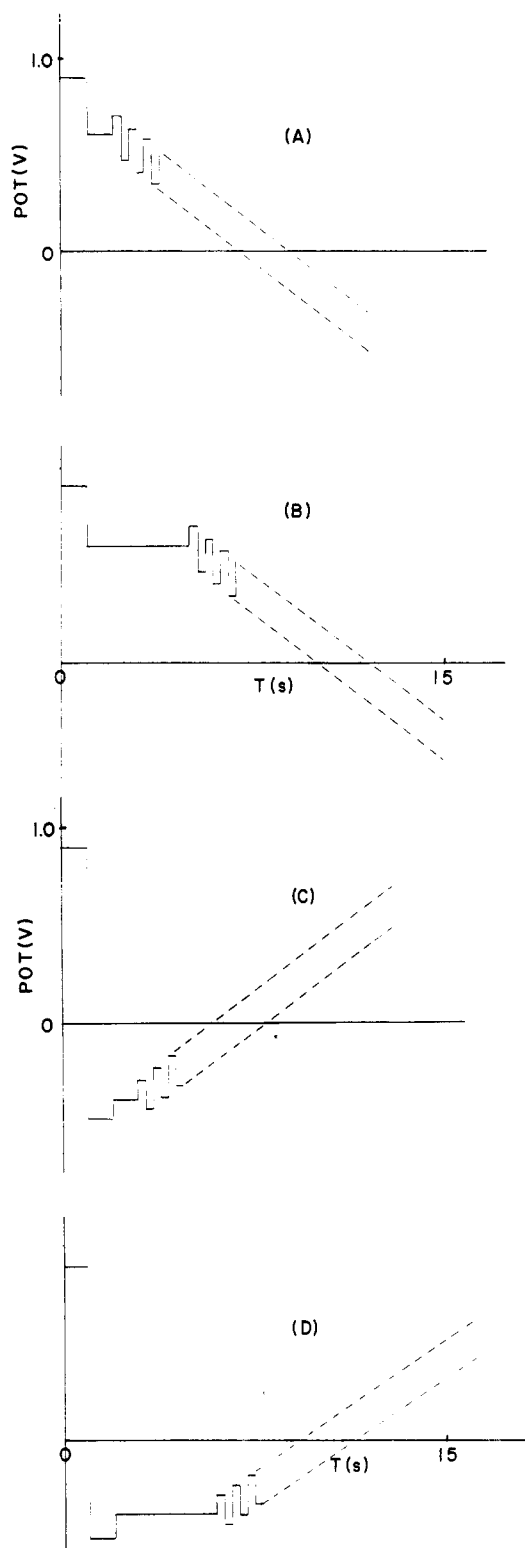
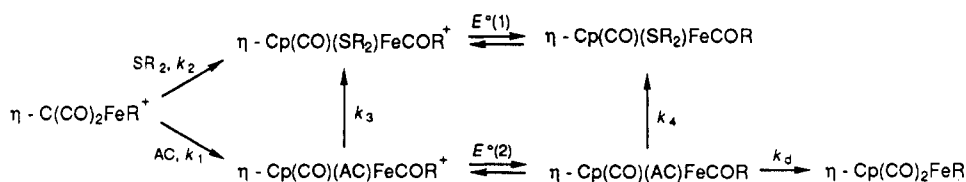


Figure 2. Schematic representations of the tailored waveforms used in square-wave voltammetry experiments. Details are discussed in the text. Initial oxidation step has a duration of 1 s for all waveforms. The second step-and-hold has a duration of 1 and 4 s in A and B, respectively. In C and D, the second step-and-hold is of 1-s duration followed by a third step-and-hold of 1 and 4 s, respectively.

segment is drawn schematically; peak amplitude is 20 mV, one cycle comprises 4 mV, and the frequency is 25 Hz. Waveforms 2A and 2B are for initial oxidation at 0.92 V followed by steps and sweeps in the negative direction. These waveforms probe primarily the chemistry in the iron(III) state. Waveforms 2C and 2D begin with the

(4) Osteryoung, J.; O'Dea, J. *Square Wave Voltammetry*. In *Electroanal. Chem. A series of Advances*; Bard, A., Ed.; Marcel Dekker: New York, 1986; Vol. 14, pp 209–308.

Scheme I

Table I. Stereoelectronic Parameters^a for SR₂, Rate Constants^b for Reactions 1-3, and E° Values^c for the $\eta\text{-Cp(CO)(SR}_2\text{)FeCOMe}^{0,+}$ Couple

thioether	θ^a	χ^b	k_5	$\log k_5$	$(k_6/k_{-6})k_7$	$\log (k_6/k_{-6})k_7$	E°
SMe ₂	79	5.7	9.7	0.99	47.9	1.68	0.123
SEt ₂	88	4.2	1.27	0.104	28.9	1.46	0.128
S(Ph)Me	88	7.3	0.141	-0.85	28.6	1.45	0.160
SBu ₂	91	3.95	0.89	-0.05	9.8	0.99	0.125
S(Ph)Et	92	6.5	0.070	-1.15	18.7	1.27	0.149
SPh ₂	97	8.8			13.7	1.14	0.207
S(t-Bu)Me	100	2.9	0.113	-0.95	13.5	1.13	0.129
S(i-Pr) ₂	107	29.5			2.46	0.39	0.119
S(t-Bu) ₂	121	0.0					

^aSee text for definition of the stereoelectronic parameters. ^bRate constants have units of $M^{-1} s^{-1}$. The standard errors associated with the rate constants are all less than 2% except for $(k_6/k_{-6})k_7$ for SMe₂, where it is within 6%. ^cThe E° values are in volts measured relative to the ferrocene/ferrocenium couple at 0.310 V.

initial oxidation followed by a step to a potential more negative than the E° for the acetone complex. Subsequent sweep is in the positive direction and probes the chemistry of both the iron(II) and iron(III) states.

We have found that initial oxidation at 0.92 V on the foot of the anodic wave of $\eta\text{-Cp(CO)}_2\text{FeMe}$ affords good results. Application of a potential greater than 1.04 V results in substantial oxidation of secondary products. Owing to the chemical irreversibility of the followup reactions, even oxidation at the foot of the anodic wave produces sufficient concentrations of oxidation products whose currents are easily measured. Experiments using ferrocene as an internal standard show that under these conditions the thioether was present everywhere in at least 5 times the concentration of $\eta\text{-Cp(AC)(CO)FeCOMe}^+$. By moving the initial oxidation potential tens of millivolts at the foot of the wave, it is possible to generate varying amounts $\eta\text{-Cp(AC)(CO)FeCOMe}^+$. On doing so we find no significant change in the shapes of the resulting SW voltammograms and therefore no change in the kinetic analysis. The results of these experiments indicate that the reaction kinetics may be treated as pseudo-first-order in $\eta\text{-Cp(AC)(CO)FeCOMe}^+$. We analyzed by computer simulation⁵ the results of SWV experiments in terms of the reaction scheme which is shown above. Finite solution resistance and heterogeneous kinetics were treated together in the framework of the Butler-Volmer equation. Diffusion coefficients, D , for all the iron complexes were taken to be the same. The heterogeneous rate constants, expressed in terms of $k^\circ/D^{1/2}$ (from the Butler-Volmer equation expressed in terms of J/nF), are typically $2.5\text{ s}^{-1/2}$ for the sulfide complexes and $1.0\text{ s}^{-1/2}$ for the acetone complex. The values of α were found to be 0.5 (based on CV measurements). The homogeneous rate constants along with the stereoelectronic properties of the thioethers and the E° values of the $\eta\text{-Cp(AC)(CO)FeCOMe}^{0,+}$ couple are listed in Table I. Figure 3 displays two SW voltammograms based on wave forms 2C and 2D for the same concentration of thioether and two different hold times along with their simulations. Figure 4 shows a series of SW voltammograms (and their simulations) also based on wave form 2C with the same hold times but different concentrations of thioether. SW voltammograms based

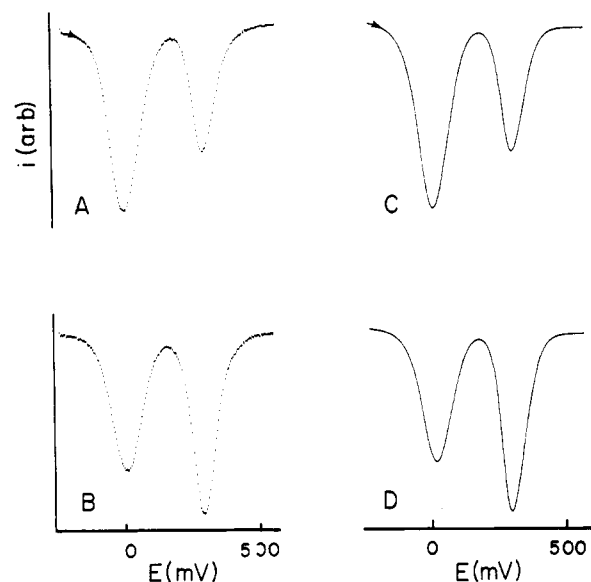


Figure 3. Experimental (A and B) and simulated (C and D) SW voltammograms for oxidation of $\eta\text{-Cp(CO)(AC)FeCOMe}$ and $\eta\text{-Cp(CO)(SPh}_2\text{)FeCOMe}$ generated by using wave forms 2C and 2D (see Figure 2), respectively. The initial concentration of SPh₂ was 7.5 mM; $k_1 = 10\text{ s}^{-1}$, $k_2 = 0$, $k_3 = 0$, $k_4 = 0.09\text{ s}^{-1}$. Initial potential of 0.92 V is held for 1 s. This is followed by a step and 1-s hold at -0.28 V, then another step (1 s for curves A and C, or 4 s for curves B and D) at -0.15 V; the square-wave segment begins here and ends at 0.60 V.

on wave forms 2A and 2B are qualitatively similar to those of Figure 3.

The pseudo-first-order rate constants for the reaction scheme were extracted from SW voltammograms by matching with the computer-simulated ones. (The rate constant, k_d , for the decomposition of $\eta\text{-Cp(AC)(CO)FeCOMe}^0$ was determined by computer simulation of a multiple-scan cyclic voltammogram for $\eta\text{-Cp(AC)(CO)FeCOMe}^{0,+}$ in acetone at -41 °C. The method is described in ref 2. The complexes, $\eta\text{-Cp(SR}_2\text{)(CO)FeCOMe}^{0,+}$ were found to be stable on the time scale of the electrochemical experiments.) A typical analysis begins with the results of wave forms 2A and 2B. The current of the cathodic waves is primarily dependent on the chemistry in the iron(III) state, allowing us to evaluate the iron(III) rate

(5) Codes are displayed in the supplementary material.

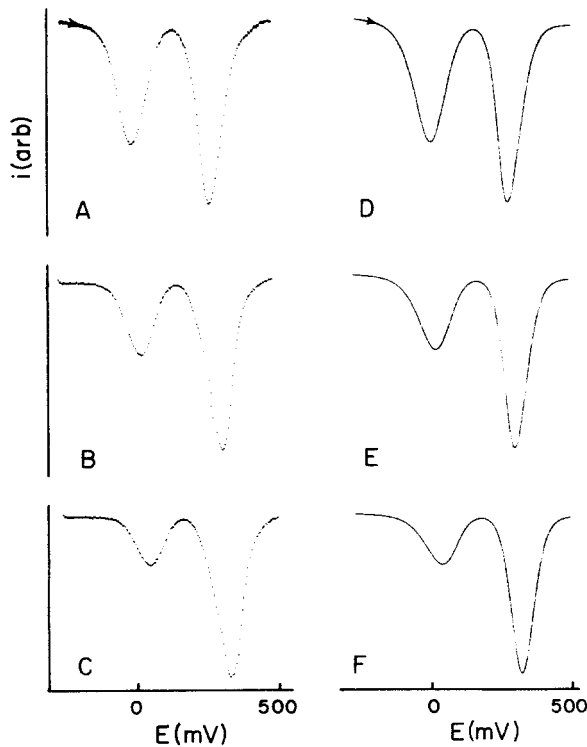


Figure 4. Experimental (A, B, and C) and simulated (D, E, and F) SW voltammograms for oxidation of η -Cp(CO)(AC)FeCOMe and η -Cp(CO)(SPh₂)FeCOMe generated by using waveform 2C (see Figure 2; the parameters of this wave form are given in Figure 3). The concentrations of SPh₂ are (A) 13.5 mM, (B) 19.5 mM, and (C) 25.5 mM. The corresponding values for k_4 were found to be 0.18, 0.25, and 0.31 s⁻¹, respectively. All other rate constants are as given in Figure 3.

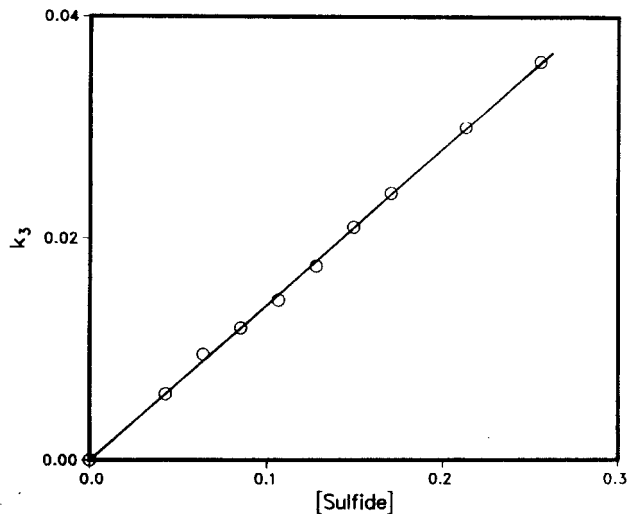


Figure 5. Plot of the observed rate constant k_3 versus [S(Ph)Me].

constant (k_3) without detailed information about the rest of the scheme. Using this information, we then evaluated the results of wave forms 2C and 2D to obtain the rate constant (k_4) for the iron(II) state. A single iteration of these steps is enough to give convergence in the rate constants.

The microscopic rate constants (k_5) were obtained from the pseudo-first-order rate constants in the standard manner. Thus, a plot of k_3 versus [SR₂] is linear with an intercept of zero and a slope that affords the second-order rate constant k_5 (Figure 5):

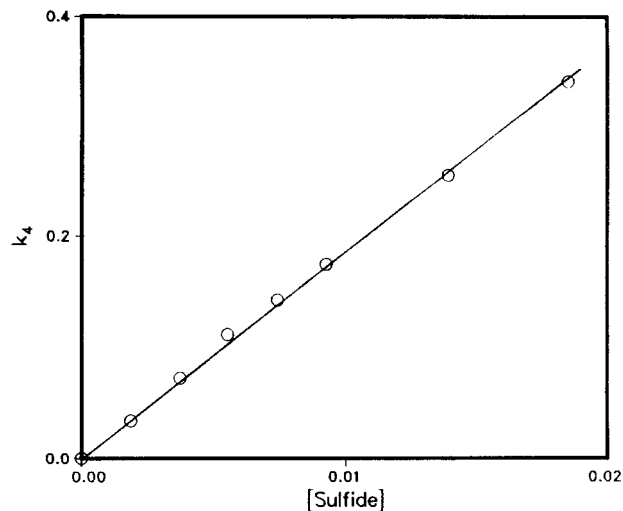
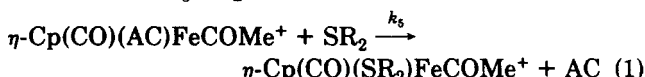


Figure 6. Plot of the observed rate constant k_4 versus [S(Ph)Et].

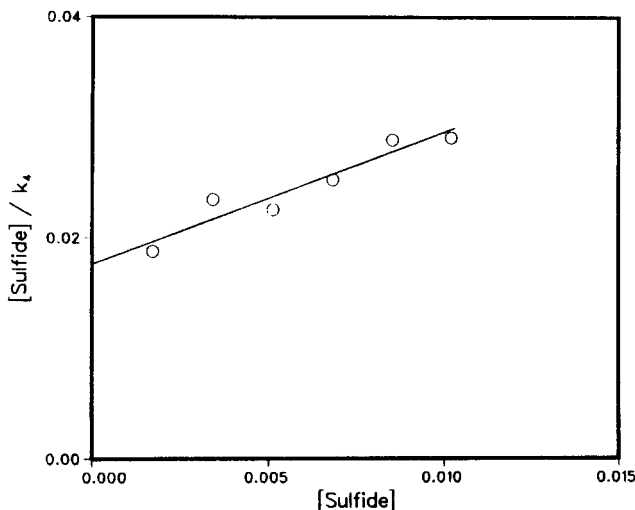
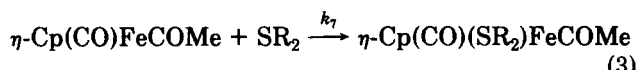
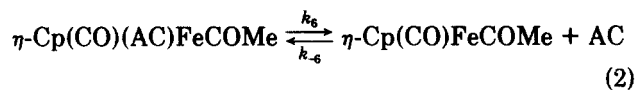


Figure 7. Plot of [SMe₂]/ k_4 versus [SMe₂].

Likewise, the plots (Figure 6) of k_4 versus [SR₂] (with the exception of the data for SMe₂) are linear with intercepts of zero and yield the values for $(k_6/k_{-6})k_7$ for the preequilibrium dissociative process shown in eqs 2 and 3. The



plot involving SMe₂ shows considerable curvature and appears to approach a constant value at high concentrations of thioether (vide infra). A plot of [SMe₂]/ k_4 versus [SMe₂] gives a straight line with an intercept and slope whose inverses give $(k_6/k_{-6})k_7$ and k_6 , respectively (Figure 7).

The use of wave forms 2A and 2B, which have different hold times after the initial oxidation, allows us to determine how much η -Cp(SR₂)(CO)FeCOMe⁺ is formed directly from the initial oxidation product (k_2) step and indirectly via the k_1 and k_3 steps. For example, if η -Cp(SR₂)(CO)FeCOMe⁺ were formed only from η -Cp(CO)₂FeMe⁺, then the concentration ratio $[\eta\text{-Cp(SR}_2\text{)CO)FeCOMe}^+]/[\eta\text{-Cp(AC)(CO)FeCOMe}^+]$ would be independent of the second hold time. On the other hand, if η -Cp(AC)(CO)FeCOMe^{0,+} is formed via the k_1/k_3 route, then the ratio will increase as function of the hold time.

We have found that the k_1 step is unimportant except at the highest concentrations of SPh_2 which, unlike the smaller and more nucleophilic thioethers, fails to react with $\eta\text{-Cp}(\text{AC})(\text{CO})\text{FeCOMe}^+$.

Discussion

The analysis of the kinetic data indicates that the substitution reactions in the iron(III) state take place via an entering ligand dependent substitution reaction. This interpretation is in accord with the results of the quantitative analysis of ligand effects (QALE,⁶ vide infra). In contrast, the substitution reaction in the iron(II) state appears to involve a preequilibrium dissociative process. This interpretation is supported by (1) the observation that the rate of reaction for SMe_2 approaches rate saturation at high concentrations of thioether, (2) the observation of kinetics that follow a two-step rate law for SPhMe at -75°C ,² and (3) the results of the QALE analysis of the kinetic data (vide infra).

The rates of the substitution reactions of $\eta\text{-Cp}(\text{AC})(\text{CO})\text{FeCOMe}^+$ are sufficiently slow at -41°C as to allow the convenient study of these reactions as a function of a wide variety of thioethers in both the iron(II) and iron(III) oxidation states. Interpretation of the kinetic data via QALE allows a comparison of the stereoelectronic factors that influence the reactivity of the two oxidation states of iron. The application of QALE does require, however, a set of parameters that describe the relative stereoelectronic properties of the thioethers. We are not aware of such a set for thioethers or a set of spectroscopic, kinetic, or thermodynamic data from which such parameters could be extracted. The situation is very different for the more common phosphorus(III) ligands, where a number of electronic parameters are available based on IR⁷ and NMR⁸ measurements and Brønsted basicity.⁹ Tolman's cone angles^{7a} are generally employed as a steric parameter.

As a solution to constructing a set of stereoelectronic parameters for the thioethers we considered the possibility that their properties are linearly related to those of the phosphorus(III) ligands. This approach appears to have provided a set of stereoelectronic parameters for SiR_3 that have allowed the interpretation of kinetic data for the reactions of allylsilanes.¹⁰ Certainly, one of the reasons for this successful transference is that the silyl groups and phosphorus(III) ligands are isostructural with identical cone angles.¹¹ Thioether ligands, in contrast, have only

(6) (a) Golovin, M. N.; Rahman, Md. M.; Belmonte, J. E.; Giering, W. P. *Organometallics* 1985, 4, 1981. (b) Rahman, Md. M.; Liu, H.-Y.; Prock, A.; Giering, W. P. *Organometallics* 1987, 6, 650. (c) Rahman, Md. M.; Liu, H.-Y.; Eriks, K.; Prock, A.; Giering, W. P. *Organometallics* 1989, 8, 1. (d) Liu, H.-Y.; Eriks, K.; Prock, A.; Giering, W. P. *Inorg. Chem.* 1989, 28, 1759. (e) Dahlinger, K.; Falcone, F.; Poe, A. J. *Inorg. Chem.* 1986, 25, 2654. (f) Poe, A. J. *Pure Appl. Chem.* 1988, 60, 1209. (g) Brodie, N. M.; Chem, L.; Poe, A. J. *Int. J. Chem. Kinet.* 1988, 20, 467. (h) Zizelman, P. M.; Amatore, C.; Kochi, J. K. *J. Am. Chem. Soc.* 1984, 106, 3771.

(7) (a) Tolman, C. A. *Chem. Rev.* 1977, 77, 313. (b) Bartik, T.; Himmeler, T.; Schulte, H.-G.; Seevogel, K. *J. Organomet. Chem.* 1984, 272, 29. See ref 9 also.

(8) Bodner, G. M.; May, M. P.; McKinney, L. E. *Inorg. Chem.* 1980, 19, 1951.

(9) (a) Allman, T.; Goel, R. G. *Can. J. Chem.* 1982, 60, 716. (b) Henderson, W. A.; Streuli, C. A. *J. Am. Chem. Soc.* 1960, 82, 5791. (c) Streuli, C. A. *Anal. Chem.* 1960, 32, 985. The most commonly used measure of the σ -donicity of phosphorus(III) ligands is the $\text{p}K_a$ values of HPR_3^+ . Since these $\text{p}K_a$ values contain a steric component that is linearly related to θ , the $\text{p}K_a$ values overestimate the σ -donicity of the smallest ligands.^{7c} We have found that χ^s values⁷ are a good measure of σ -donicity for trialkyl-, mixed alkyl/aryl-, and triarylpophosphines.

(10) Panek, J.; Eriks, K.; Prock, A.; Giering, W. P. Submitted for publication.

(11) Ilyanitov, N. S. *Koord. Khim.* 1985, 11, 1171.

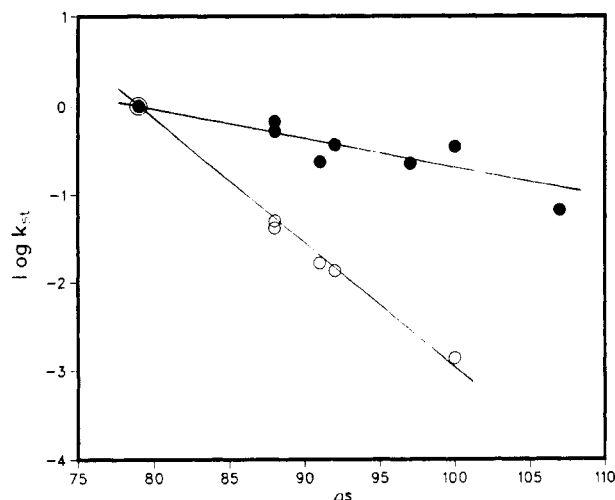


Figure 8. Steric profiles for the entering ligand-dependent substitution reaction (eq 1, open circles) and the addition of SR_2 to $\eta\text{-Cp}(\text{CO})\text{FeCOMe}$ (eq 3, filled circles). The values of $\log k_{st}$ were obtained for each ligand by subtracting from the experimental $\log k$ the value from eq 4 or 5 leaving out the θ term. The scales of $\log k_{st}$ were adjusted so as to set the $\log k_{st}$ for the SMe_2 complexes to zero.

two pendent groups and a nonbonding pair of electrons. It is certainly possible that the thioethers might behave as π -bases.¹² In addition, the π - acidity of thioethers might be greater than that of phosphorus(III) ligands by virtue of the greater electronegativity of sulfur. As a first step toward constructing a set of stereoelectronic parameters for thioethers, we assumed that for the dialkyl, mixed alkyl/aryl, and diaryl thioethers the M-S bonding was analogous to the M-P bonding for trialkyl-, mixed alkyl/aryl-, and triarylpophosphines. Accordingly, we used the fractional χ and θ values⁷ for the trisubstituted phosphorus(III) ligands to calculate a σ -electronic parameter χ^s and a steric parameter θ^s for the thioethers (Table I). We do not have fractional values for θ or χ for the nonbonding pair of electrons; however, we assumed them to be constant and we ignored their contribution to the total θ^s and χ^s of the thioethers. A measure of the validity of this approach lies in the quality of the QALE analysis that results from treatment of the kinetic data. If the M-S bonding differs significantly from M-P bonding, then there is no reason to believe that the aforementioned parameters would yield meaningful correlations.

The following observations suggest that the transference of the stereoelectronic parameters from phosphorus(III) to sulfur is valid. First, there is an excellent correlation ($r = 0.994$) between χ^s , θ^s , and $\log k_5$ for the entering ligand-dependent substitution reaction in the iron(III) state (eq 4, standard errors are given in parentheses). Second,

$$\log k_5 = (-0.332 \pm 0.023)\chi^s - (0.137 \pm 0.005)\theta^s + (13.66 \pm 0.61) \quad (4)$$

the results of the QALE analysis are intuitively reasonable and parallel those obtained for entering ligand-dependent substitution reactions involving incipient phosphorus(III) ligands. The rate of reaction 1 is enhanced by increasing Lewis basicity (smaller χ^s values) of the thioether while the rate is retarded by increasing steric bulk (larger θ^s).

In reaction 1, steric effects are continuously operative for all the thioethers used in this study (Figure 8), whereas many analogous reactions involving PR_3 as the entering

(12) Basolo, F.; Pearson, R. G. *Mechanism of Inorganic Reactions. A Study of Metal Complexes in Solution*, 2nd ed.; Wiley: New York, 1967.

ligand exhibit steric thresholds. We speculate that the absence of a steric threshold for the thioethers reflects a crowded transition state with an Fe–S bond that is shorter than the corresponding Fe–P bond. The steric sensitivity (coefficient of the θ^s term in eq 4) is similar to that observed for reactions involving PR_3 and cyclopentadienyl complexes. This steric inhibition is undoubtedly the reason the larger ligands SPh_2 , $\text{S}(i\text{-Pr})_2$, and $\text{S}(t\text{-Bu})_2$ fail to react via the entering ligand-dependent pathway in the iron(III) state. (The size of the most basic and largest thioether, $\text{S}(t\text{-Bu})_2$, apparently prevents this thioether from reacting with any of the complexes.)

Although SPh_2 does not react with $\eta\text{-Cp}(\text{AC})(\text{CO})\text{FeCOMe}^+$, it does react with a species formed immediately after oxidation of $\eta\text{-Cp}(\text{CO})_2\text{FeMe}$. Thus, at high concentrations of SPh_2 with wave form 2A the cathodic wave for $\eta\text{-Cp}(\text{SPh}_2)(\text{CO})\text{FeCOMe}^+$ is observed. With wave form 2B, which incorporates an intermediate hold of longer duration, the ratio of $[\eta\text{-Cp}(\text{SPh}_2)(\text{CO})\text{FeCOMe}^+]/[\eta\text{-Cp}(\text{AC})(\text{CO})\text{FeCOMe}^+]$ remains the same, thereby showing that the thioether complex is not forming from the acetone complex. These results once again appear to be consistent with the generation of a highly reactive electrophile something akin to $\eta\text{-Cp}(\text{CO})\text{FeCOMe}^+$ immediately after the oxidation of $\eta\text{-Cp}(\text{CO})_2\text{FeMe}$.

The substitution reactions in the iron(II) state follow second-order kinetics with the exception of SMe_2 . We believe that the mechanism is a preequilibrium dissociative process as described in eqs 2 and 3. This interpretation of the data is consistent with our observation that the reaction between $\text{S}(\text{Ph})\text{Me}$ and $\eta\text{-Cp}(\text{AC})(\text{CO})\text{FeCOMe}^+$ follows a two-term rate law at -75°C . Only for the most reactive thioether, SMe_2 , is the rate of the second step sufficiently fast as -41°C to force the reaction toward rate saturation at high concentrations of thioether. From the SMe_2 data we calculated a first-order rate constant (k_6) for the dissociation of acetone from $\eta\text{-Cp}(\text{AC})(\text{CO})\text{FeCOMe}$ to be 0.84 s^{-1} with a standard error of $\pm 0.13\text{ s}^{-1}$. It is interesting to note that the rate of decomposition of $\eta\text{-Cp}(\text{AC})(\text{CO})\text{FeCOMe}$ (presumably back to $\eta\text{-Cp}(\text{CO})_2\text{FeMe}$) is only $0.22 \pm 0.05\text{ s}^{-1}$. Hence, the decomposition of $\eta\text{-Cp}(\text{CO})(\text{AC})\text{FeCOMe}$ and the formation of $\eta\text{-Cp}(\text{SMe}_2)(\text{CO})\text{FeCOMe}$ apparently do not share the same reaction pathway.

The application of QALE to the kinetic data for reactions 2 and 3 shows that the coefficient of the electronic term (eq 5) is statistically indistinguishable from zero,

$$\log(k_6/k_{-6})k_7 = (0.033 \pm 0.033)\chi^s - (0.037 \pm 0.008)\theta^s + (4.52 \pm 0.91) \quad (5)$$

whereas there is a small but significant inhibiting steric component. (At this stage, we do not know if the smallness of electronic coefficient is the result of being near an electronic isokinetic point.) The results of QALE, coupled with the kinetic analysis, indicate that we are dealing with the coordinatively unsaturated complex $\eta\text{-Cp}(\text{CO})\text{FeCOMe}$. This complex appears to be a highly reactive electrophile, showing little electronic discrimination between the thioethers. The steric effect is 4-fold less than that observed in the substitution reaction in the iron(III) state (Figure 8). We interpret this result as being consistent with addition to a more flexible five-coordinate complex $\eta\text{-Cp}(\text{CO})\text{FeCOMe}$ as compared to addition to the less flexible and more congested $\eta\text{-Cp}(\text{AC})(\text{CO})\text{FeCOMe}^+$.

It seems likely that the addition of a thioether to $\eta\text{-Cp}(\text{CO})\text{FeCOMe}$ involves an early transition state with a long and weak Fe–S bond. Since the transition state shows steric effects, then the more compact $\eta\text{-Cp}(\text{SR}_2)(\text{CO})\text{Fe}$

COMe should also show steric effects. Indeed, analysis of the E° values of the $\eta\text{-Cp}(\text{SR}_2)(\text{CO})\text{FeCOMe}^{0,+}$ couple shows such an effect. Steric effects may either decrease or increase the E° values of the $\eta\text{-Cp}(\text{SR}_2)(\text{CO})\text{FeCOMe}^{0,+}$ couple. If steric destabilization is greater in the reduced state, then the oxidation will be easier for complexes containing larger ligands. In contrast, if steric destabilization is greater in the oxidized state, then the complexes will be more difficult to oxidize as the sizes of the ligands increase. Inspection of the E° values displayed in Table I shows that steric effects are operative and that steric destabilization is greater in the oxidized state. For example, the smallest but not the most basic thioether (SMe_2) exhibits the most second most negative E° value. On the other hand, one of the most basic and largest ligand ($\text{S}(t\text{-Bu})\text{Me}$) exhibits an E° value 6 mV more positive. QALE analysis of the E° values (excluding $\text{S}(i\text{-Pr})_2$) gives the following relationship between E° and the stereoelectronic parameters for the $\eta\text{-Cp}(\text{SR}_2)(\text{CO})\text{FeCOMe}^{0,+}$ couple:

$$E^\circ = +(0.0126 \pm 0.0014)\chi^s + (0.0021 \pm 0.0004)\theta^s - (0.114 \pm 0.043) \quad (r = 0.98) \quad (6)$$

The E° value for the $\eta\text{-Cp}(\text{S}(i\text{-Pr})_2)(\text{CO})\text{FeCOMe}^{0,+}$ does not fit the above pattern. At 0.119 V this complex is much too easily oxidized. This deviant behavior is currently under investigation.

It is important to note that $\eta\text{-Cp}(\text{SR}_2)(\text{CO})\text{FeCOMe}^{0,+}$ show steric effects in both states, whereas the analogous complexes $\eta\text{-Cp}(\text{PR}_3)(\text{CO})\text{FeCOMe}^{0,+}$ do not show steric effects based on evaluations of E° values and Fe–P bond lengths. For example, the QALE analysis of the E° values for complexes containing PEt_3 , PPh_3 , PPhEt_2 , PPh_2Et , PBu_3 , PPhMe_2 , PPh_2Me , $\text{P}(i\text{-Bu})_3$, PPh_2Cy , and PCy_3 gives the following result, which shows little dependence on ligand size:

$$E^\circ = +(0.015 \pm 0.001)\chi + (0.0003 \pm 0.0003)\theta - (0.161 \pm 0.055) \quad (7)$$

The virtual absence of steric effects can be interpreted in terms of no steric effects in either the reduced or oxidized state or of equal and canceling steric effects in the two states. The latter seems highly unlikely since there are probably changes in ligand–metal bond lengths accompanying changes in oxidation state. Thus, we believe that there are no steric effects operative for those phosphorus(III) complexes even though the size of the ligands spans a range in cone angle from 122° to 170° . The observation of steric effects in the sulfur complexes and lack of steric effects in the phosphorus(III) complexes means that steric effects are not continuously operative; this is independent support for the concept of the steric threshold.

Experimental Section

Electrochemistry. Experiments were performed on a computer-controlled EG&G PAR Model 273 potentiostat using the commands of the HEADSTART program provided by EG&G PAR. A one-compartment cell with a three-electrode configuration was used. A platinum wire was used as pseudoreference electrode. The concentration of $\eta\text{-Cp}(\text{CO})_2\text{FeMe}$ was about 6.0 mM ; experiments using ferrocene as an internal standard showed no more than a 10% conversion of the $\eta\text{-Cp}(\text{CO})_2\text{FeMe}$ to $\eta\text{-Cp}(\text{CO})(\text{AC})\text{Fe}(\text{COMe})^+$ upon oxidation. All E° values were referenced to the $\eta\text{-Cp}(\text{CO})(\text{AC})\text{FeCOMe}^{0,+}$ couple at -0.016 V measured against the ferrocene/ferrocenium couple at 0.310 V . The electrolyte was a solution of acetone containing 0.1 M LiClO_4 . The solutions were cooled to -41°C in an acetonitrile slush bath. The preparation and purification of reagents were described earlier.² Since we had shown previously² that repeated distillation of

thioanisole did not affect the kinetics of the reactions, we used the thioethers as they were received from commercial sources. It is necessary to shield the cell from room light, otherwise reactions in the bulk produce unidentified electrochemically active species.

Computer Simulation. The code for the computer simulation of the SW voltammograms is based on the methodology described earlier² except that here square waves are employed. Thus in the numerical analysis we define the potential by dividing each square wave period into a sufficiently fine net, typically 14 equal time segments. Potential is held constant for seven time steps and then is stepped to the next value for another seven steps. Current output is computed as the difference between currents at the seventh and fourteenth segment for each period. This simulates the experimentally measured difference in currents between the ends of the first and second half of each square wave. Sweep rate was 0.100 V s⁻¹, corresponding to a square-wave frequency of 25 Hz and square-wave length of 4.00 mV. The rest of the computation proceeds along the lines discussed in our earlier paper.² Numerical computation was done using the Adams-Moulton method, with predictor and corrector of order 1 and 2, respectively.¹³ As a check of the computation, we examined the case

of initial uniform concentration of oxidized acetone complex with either no or full conversion to the sulfide complex and compared the simulation results with the numerical solution obtainable in terms of Laplace transforms.⁴ We find for a range of heterogeneous rate constant $k_0/D^{1/2}$ from 30 s^{-1/2} (virtually Nernstian) down to 0.8 s^{-1/2} (below the present range of application) that the results are in good agreement, giving the same shifts in peak potential and the same half-widths and current ratios. The values for the heterogeneous rate constants stated above were found by means of matching experimental and simulated half-widths of the current peaks. These were verified by comparing experimental and computed differences in peak potentials as determined by cyclic voltammetry experiments on these complexes. The code for both the simulation and the Laplace transform solution is provided in the supplementary material (see the paragraph at the end of the paper).

Acknowledgment. We gratefully thank the donors of the Petroleum Research Fund, administered by the American Chemical Society, and the Graduate School of Boston University for support of this research. We thank Professor Janet Osteryoung for helpful comments.

(13) Shampine, L. F.; Gordon, M. K. *Computer Solution of Ordinary Differential Equations*; W. H. Freeman: San Francisco, 1975.

Supplementary Material Available: Code for both the simulation and the Laplace transform solution (4 pages). Ordering information is given on any current masthead page.

Five- and Six-Membered Exo-Cyclopalladated Compounds of *N*-Benzylideneamines. Synthesis and X-ray Crystal Structure of $[\text{PdBr}\{p\text{-MeOC}_6\text{H}_3(\text{CH}_2)_2\text{N}=\text{CH}(2,6\text{-Cl}_2\text{C}_6\text{H}_3)\}\{\text{PPh}_3\}]$ and $[\text{PdBr}\{\text{C}_6\text{H}_4\text{CH}_2\text{N}=\text{CH}(2,6\text{-Cl}_2\text{C}_6\text{H}_3)\}\{\text{PEt}_3\}_2]$

Joan Albert, Montserrat Gómez, Jaume Granell, and Joaquim Sales*

Departament de Química Inorgànica, Universitat de Barcelona, Diagonal 647, 08028 Barcelona, Spain

Xavier Solans

Departament de Cristallografia i Mineralogia, Universitat de Barcelona, Martí i Franquès, s/n 08028 Barcelona, Spain

Received August 14, 1989

The reaction of *N*-(2,6-dichlorobenzylidene)amines, 2,6-Cl₂C₆H₃CH=N(CH₂)_nC₆H₄-*p*-R (*n* = 1, 2; R = H, MeO), with Pd(AcO)₂ in refluxing acetic acid has been studied. With *N*-benzylidenebenzylamines (*n* = 1) exo five-membered derivatives were obtained. From *N*-benzylidene(2-phenylethyl)amines (*n* = 2) endo five-membered cyclopalladated compounds were formed by oxidative addition of C-Cl bonds of the ligand to Pd(0) formed in situ. Under milder conditions (acetic acid at 80 °C) the exo six-membered compound [Pd(AcO){*p*-MeOC₆H₃(CH₂)₂N=CH(2,6-Cl₂C₆H₃)}]₂ was obtained. All exo derivatives contain the imine ligand in the syn form. By reaction with PR₃ (R = Et, Ph), monophosphine complexes [PdX(C=N)(PR₃)] and bisphosphine derivatives [PdX(C=N)(PR₃)₂], where the Pd-N bond has been broken, can be obtained. [PdBr{*p*-MeOC₆H₃(CH₂)₂N=CH(2,6-Cl₂C₆H₃)}\{\text{PPh}_3\}] (6f) crystallizes in the monoclinic space group *P*2₁/*n* with *a* = 20.321 (4) Å, *b* = 12.561 (3) Å, *c* = 12.608 (3) Å, β = 97.50 (2)°, and *Z* = 4. The exo six-membered ring displays a boat conformation with Pd and C(7) atoms out of the plane defined by the remaining atoms. [PdBr{C₆H₄CH₂N=CH(2,6-Cl₂C₆H₃)}\{\text{PEt}_3\}₂] (9c) has been characterized by X-ray crystallography; it crystallizes in the monoclinic space group *P*2₁/*a* with *a* = 45.352 (6) Å, *b* = 8.884 (2) Å, *c* = 7.556 (2) Å, β = 99.02 (3)°, and *Z* = 4. The Pd atom has a roughly planar coordination, and the imine ligand is in the anti form.

Introduction

Cyclometalation reactions are a rapidly growing area of organometallic chemistry, in particular cyclopalladation of N-donor ligands.¹ This process represents one of the

classic ways to activate C-H bonds in heterosubstituted organic molecules. Cyclopalladated compounds are valuable intermediates for regio- and stereoselective organic synthesis. Carbonylation, vinylation, and halogenation of organic compounds have been reported.² The insertion of symmetric and asymmetric alkynes at several cyclometalated complexes has been recently studied.³ In many

(1) (a) Bruce, M. I. *Angew. Chem., Int. Ed. Engl.* 1977, 16, 73. (b) Omae, I. *Chem. Rev.* 1979, 79, 287. (c) Newkome, G. R.; Puckett, W. E.; Gupta, V. K.; Kiefer, G. E. *Chem. Rev.* 1986, 86, 451. (d) Omae, I. *Coord. Chem. Rev.* 1988, 83, 137. (e) Dunina, V. V.; Zalevskaya, O. A.; Potatov, V. M. *Russ. Chem. Rev.* 1988, 57, 250.

(2) Ryabov, A. D. *Synthesis* 1985, 233.